Hindawi
Journal of Chemistry
Volume 2022, Article ID 1125877, 15 pages
https://doi.org/10.1155/2022/1125877

Research Article

Optimized Removal of Hydroquinone and Resorcinol by Activated Carbon Based on Shea Residue (*Vitellaria paradoxa*): Thermodynamics, Adsorption Mechanism, Nonlinear Kinetics, and Isotherms

Liouna Adoum Amola,[1] **Theophile Kamgaing**,[1] **Rufis Fregue Tiegam Tagne**,[2] **Cyrille Donlifack Atemkeng**,[1] **Idris-Hermann Tiotsop Kuete**,[1] **and Solomon Gabche Anagho**[1]

[1]*Research Unit of Noxious Chemistry and Environmental Engineering, Department of Chemistry, University of Dschang, P.O. Box 67, Dschang, Cameroon*
[2]*Department of Paper Sciences and Bioenergy, University Institute of Wood Technology, University of Yaounde I, Mbalmayo, Cameroon*

Correspondence should be addressed to Theophile Kamgaing; theokamgaing@yahoo.fr

Received 13 November 2021; Revised 17 December 2021; Accepted 22 December 2021; Published 17 January 2022

Academic Editor: Yuanjuan Bai

The present work demonstrates the adsorption of hydroquinone (HQ) and resorcinol (R) by activated carbon based on shea residue (*Vitellaria paradoxa*). The adsorbent was prepared chemically by impregnation with sulfuric acid and coded by the acronym CAK-S. The central composite design (CCD) was used to optimize the main factors that influence the adsorption of HQ or R by activated carbon such as the initial concentration, the pH of the solution, the contact time, and the mass of the carbon on the expected response, which is the adsorbed quantity of the target pollutants. The optimal conditions obtained from the statistical analysis are as follows: concentration of 158 mg/L, pH 3, time of 120 min, and mass of 50 mg for the adsorption of HQ and concentration of 180 mg/L, pH 3, time of 86 min, and mass of 118 mg for the adsorption of R. The maximum quantities of HQ and R adsorbed are 45.02 mg/g and 33.65 mg/g, respectively. The analysis of variance (ANOVA) showed a good relationship between the variables involved with the coefficients of determination $R^2 = 98.69\%$ for the adsorption of hydroquinone and $R^2 = 90.55\%$ for that of resorcinol, which means that the model is more suitable to express the adsorbed amount according to the four optimized parameters. The experimental data obtained under these optimal conditions were simulated with two and three parameter nonlinear isotherm models as well as kinetic models. The results show that Elovich kinetic model better describes the adsorption of HQ and R, indicating chemisorption with heterogeneous active sites on the surface of CAK-S. Temkin's two-parameter model shows that adsorption occurs on heterogeneous surfaces with a nonuniform adsorption energy distribution at the surface and Sips's three-parameter model confirms the heterogeneity of the surface with a localized adsorption of HQ or R by CAK-S. The thermodynamics study has shown that the adsorption is endothermic ($\Delta H^0 > 0$) and spontaneous ($\Delta G^0 < 0$).

1. Introduction

Environmental pollution remains as one of the major problems arising from technological development. Phenolic compounds and their derivatives are recognized as pollutants [1]. They are released into the environment during their production and use. They mainly come from discharges from textile, petrochemical, petroleum refinery, rubber, dye, plastic, pharmaceutical, and cosmetic industries [2, 3]. Several phenolic derivatives such as hydroquinone (HQ) and resorcinol (R) have been recognized as being dangerous pollutants due to their potential toxicity [4]. Wastewater

laden with HQ and R is harmful to the environment in general and to the aquatic environment in particular [4, 5] because these compounds dissolve and can easily infiltrate the environment. Although the carcinogenic effects of HQ and R in humans are controversial, these compounds cause acute toxicity in several organs such as the kidneys and stomach [1] and are suspected to be endocrine disruptors. The human body exposure threshold is 0.5 mg/L [6] for HQ and 10 mg/L for R [7]. Therefore, wastewater containing these pollutants beyond these standards, respectively, must be subjected to treatment before discharge. Thus, many processes for treating water loaded with phenolic derivatives have been recommended. These include conventional physical, chemical, or biological processes such as chemical oxidation, chemical reduction, chemical precipitation, adsorption, ion exchange, solvent extraction, reversed osmosis, and aerobic and anaerobic biodegradation [8–14]. The application of some of these methods is restricted not only because of technical and economic constraints but also by the fact that some of them are not accessible to low-income developing countries. It is in this logic that, for some time, researchers have been investigating the development of less expensive methods, including adsorption on adsorbents at a lower cost [15–17]. These less expensive adsorbents can be simple biomasses or activated carbons prepared from agroindustrial residues [18–20]. Tropical Africa is full of potential valuable fruit species which are not only abundant but also available almost round the year. They tend to generate large amounts of waste residue which can be used in the preparation of activated carbons. An example of such a residue is nuts from the plant *Vitellaria paradoxa*. It is widely distributed in southern Chad.

Nowadays, the method of optimization by experimental design is increasingly appealing to researchers because it permits the extraction of maximum information with a minimum of simulation results. One of the adsorption optimization methods is the response surface methodology, which is an efficient statistical tool, making it possible to explain interactions independent of operating parameters [21–23]. The central composite design was used in this work to optimize the factors that affect the adsorption of HQ and R from solution. These factors include initial concentration, the pH of the solution, the contact time, and the mass of carbon on the response which is the adsorbed quantity of HQ or R. These experimental quantities can be simulated by kinetic or isotherm models. Nowadays, to properly describe and model the kinetic and isotherm adsorption, two methods exist: the nonlinear method and the linear method. Recent works have shown that nonlinear regression produces very satisfactory results compared to linear regression [24, 25]. Thus, for the nonlinear regression, the selection of the error functions showed a remarkable change in terms of the values of the constants linked to the models studied [26, 27]. So, nonlinear regression is the best option. The objective of this work is threefold. We propose (i) valorizing the shea residue (already calcined) of Chadian origin by examining its adsorption capacity on HQ and R in batch mode, (ii) optimizing the operating parameters of adsorption by response surface methodology, and (iii) modeling the kinetic, equilibrium, and adsorption isotherms by the nonlinear method. We also evaluate the thermodynamic processes that accompany it. The interest of this work is the efficient removal of organic pollutants by activated carbon based on agricultural by-products for a sustainable use of local biomass.

2. Materials and Methods

2.1. Chemicals. Hydroquinone and resorcinol are isomers with a molar mass of 110.11 g/mol. They were purchased with a purity greater than 99% from Sigma-Aldrich alongside all the other chemicals used in this work. The structures and some chemical properties of HQ and R are shown in Table 1.

2.2. Preparation of the Adsorbent. The procedure for preparing the activated carbon is that described in our previous work [28]. The shea nut shells (CNK) were collected in Baktchoro in the Division of Tandjilé-Ouest, Province of Tandjilé, Chad. Once collected, they were first washed with tap water to remove the rest of the pulp and any other form of impurities and then dried in an oven at 105°C for 24 hours to dehydrate them. They were crushed and the sizes of 0.5–2 mm were kept. A mass of 20 g of shea nut shells was impregnated with 40 mL of sulfuric acid (H_2SO_4) with concentration of 3.5 mol/L. The mixture was stirred for 24 hours to ensure reaction between the activating agent and the biomass and then filtered and dried in an oven at a temperature of 105°C for 1 hour. The impregnated materials were carbonized in a reactor (HERAEUS) at 700°C at a constant rate of 6°C/min and a residence time of 120 minutes. The carbonized material was washed to remove residual acid until it attained the pH value of the water used in washing. It was oven-dried at 105°C, crushed, and sieved to obtain particles with a diameter of less than 200 μm. The activated carbon obtained from shea nuts by impregnation with sulfuric acid was coded CAK-S.

2.3. Characterization of Activated Carbon. The use of a material in adsorption deserves broad knowledge of its physicochemical and structural properties. The activated carbon produced was characterized. These characterizations focused on energy dispersive X-ray spectrometry (EDX), scanning electron microscopy, determination of porous structure by nitrogen adsorption at 77 K by coupling the Brunauer–Emmett–Teller (BET) method to that of Barret–Joyner–Halenda (BJH), the quantification of surface chemical functions by the Boehm method, and the pH at the point of zero charge (pHpzc). The crystalline or amorphous structure of the activated carbon was analyzed by means of X-ray diffraction. The analysis was carried out on a STOE Stage device (STOE & Co. GmbH, Darmstadt, Germany) with a Cu K α1 radiation ($\lambda = 1.54056$°A, 40 kV, 30 mA).

2.4. Batch Mode Adsorption Studies. A 1000 mg/L stock solution of hydroquinone and resorcinol was prepared by dissolving 1.01 g each in 1 L of distilled water. Standards

Table 1: Chemical structures and some properties of hydroquinone and resorcinol.

Some chemical structures	Hydroquinone	Resorcinol
Chemical structure	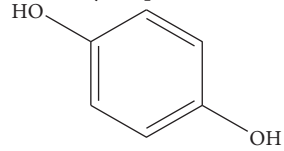	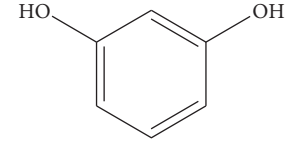
Molecular formula	C_6H_4-1,4(OH)	C_6H_4-1,3(OH)
λ_{max} (nm)	276	274
Solubility in water (25°C)	73 g/L	717 g/L
pKa	9.96	9.26

were then obtained by dilution of the stock solution. The pH of the solution was adjusted with 0.1 mol/L solution of NaOH and 0.1 mol/L solution of HCl, using a Mettler Toledo brand pH meter. Batch adsorption was performed following the central composite design matrix. A mass, m (g), of activated carbon was put in contact with 30 mL of a solution of hydroquinone or resorcinol of initial concentration, C (mg/L). The mixture obtained was placed on an agitator at a speed of 150 rpm for a contact time, t (min), at room temperature of 25°C. At equilibrium, the mixture was filtered; the filtrate obtained was analyzed by ultraviolet visible spectrophotometry (UV-Vis) at a wavelength of 276 nm and 274 nm, respectively, for hydroquinone and resorcinol. The amount adsorbed per gram of activated carbon was calculated using the following equation:

$$Q_e = \frac{C_i - C_e}{m} V, \tag{1}$$

where Q_e (mg/g) is the adsorption capacity, m (g) is the mass of activated carbon, C_i and C_e (mg/L) are the initial and equilibrium concentrations, respectively, and V (L) is the volume of the pollutant solution used.

2.5. Response Surface Methodology and Statistical Analysis of the Data. The response surface methodology is a statistical analysis tool that predicts and develops a regression model for quantitative data obtained during an experiment [22]. The model equations predict and optimize the operating conditions of the process. This makes it possible to understand the mutual dependence of the variables and to know the variables that govern the experimental system. In this work, the response surface methodology was employed to assess the interdependence of operating variables such as the initial concentration of hydroquinone or resorcinol, the pH of the solution, the contact time, and the mass of activated carbon on the adsorption process. The central composite design was used to optimize the process [22]. For four independent variables and four chosen central points, the CCD generates 28 experiments according to the following equation:

$$N = 2^k + 2k + k_c = 2^4 + 2 * 4 + 4 = 28, \tag{2}$$

where N is the total number of experiments, k is the number of factors studied, and k_c is the number of points in the center which allows measuring the reproducibility of data.

These variables were coded as such: adsorbate concentration (A: 20–180 mg/L), solution pH (B: 2–8), contact time (C: 60–120 min), and mass of activated carbon (D: 50–250 mg). The response, Y, observed is the amount of HQ or R adsorbed on CAK-S carbon. The levels of the experimental values were also coded as follows: −1, the small value, 0, the value in the center, and +1, the upper value. This unique encoding is defined from the one-to-one transformation defining the value x_i of equation (3) [29]. All coded variables are shown in Table 2.

$$x_i = \frac{L_i - L_0}{\Delta L}, \tag{3}$$

where x_i is the value of the independent variable, L_i is the value of variable i, L_o is the value at the central point, and ΔL is the step.

The 28 experiments represent a system which translates the quadratic model (equation (4)) to study the interactions between the variables [30].

$$Y = \beta_0 + \sum_{i=1}^{n} \beta_i x_i + \sum_{i=1}^{n} \beta_{ii} x_i^2 + \sum_{i=1}^{n} \sum_{j=1}^{n} \beta_{ij} x_i x_j + \varepsilon, \tag{4}$$

where Y is the predicted response, β_0 is the constant of the quadratic equation, β_i is the linear coefficient, β_{ii} is the quadratic coefficient, β_{ij} is the coefficient of the interaction between the variables, x_i and x_j are the coded values of the factors, and ε is the uncertainty between measured and predicted values.

2.5.1. Validation of the Statistical Model. To complete the statistical analysis of the experimental data, STATGRAPHIC Plus 5.0 software was used. This software statistically evaluates according to the following criteria: (a) each factor must present a p value, that is, the value of the probability smaller than 5%, with a confidence limit of 95%, (b) the value of regression coefficient R^2 must be as close as possible to 1, which means that the experimental values and the predicted values are close to each other, (c) the t-test must be significant ($p < 0.05$), which means that the model adequately describes the experimental data, and eventually (d) the proximity between the data of the predicted points and the data of the experimental points must present a normal distribution to validate the hypothesis made by the analysis of variance (ANOVA) [22].

Table 2: Matrix of coded variables.

Variables	Symbols	Units	Coded variables	Variables levels		
				−1	0	+1
Concentration	C_0	(mg/L)	A	20	100	180
pH	pH	—	B	2	6	10
Time	t	(min)	C	30	75	120
Mass	m	(mg)	D	50	150	250

2.6. Kinetic and Isothermal Adsorption Equilibrium. To understand the mechanism that governs the binding of HQ or R on CAK-S, the experimental data were applied to nonlinear kinetic models including the pseudo-first-order model, pseudo-second-order model, Elovich kinetic model, and the intraparticle model. In addition, for the adsorption isotherm of HQ or R, the two-parameter and three-parameter nonlinear models were simulated with the experimental data (Table 3).

2.7. Nonlinear Method and Analysis of Error Functions. The purpose of nonlinear regression is to adjust a set of values in order to bring the experimental curves closer to the predictions. The difference between the linear and nonlinear methods is that the latter is iterative and based on an algorithm and error functions [40, 41]. Table 4 shows the mathematical expressions of the error functions used in this work.

3. Results and Discussion

3.1. Characterization of Activated Carbon. The detailed characterizations of CAK-S carbon have been reported in our previous work [28]. It was found that this activated carbon has a specific surface area of 490.62 m^2/g, a microporous surface area of 570.56 m^2/g, and a mesoporous surface area of 10.77 m^2/g, as well as a pH at the zero charge point of 6.37. The X-ray diffraction of the material, which was not included in our previous work, is presented here (Figure 1). We observe in Figure 1 a broad peak around 20° for the two spectra corresponding to the amorphous structure of carbon. The spectra show that both raw and calcined shea nut shells have an amorphous structure. This amorphous structure is a preferred property of well-defined adsorbents [26].

Figure 2 shows the FTIR spectra recorded in the region of 3500 and 700 cm^{-1}. Before adsorption of pollutants HQ and R by CAK-S, a signal at 3395.41 cm^{-1} is observed on the spectrum attributable to the O–H group of phenols and alcohols; this would be due to the presence of hydroxyl groups in the water chemisorbed [14] on CAK-S. Other peaks were observed: a peak at 2368.65 cm^{-1} attributable to O = C = O and another at 1731.65 cm^{-1} corresponding to the C = O group of esters and lactones. We also observed a peak at 1040.36 cm^{-1} corresponding to the C–O group of alcohols and ethers and the same group at 1257.96 cm^{-1} characteristic of carboxylic acids. A shift of these peaks is observed on the spectra of CAK-S after adsorption (HQ/CAK-S and R/CAK-P), which proves that the absorption band of these two phenolic compounds was involved. The change in absorption band is much more observed on the hydroxyl, carboxylate, and C–O groups of CAK-S.

3.2. Experimental Design Using the Central Composite Design

3.2.1. Development of Quadratic Model Equations. The optimization process is based on a central composite design involving three main steps: (1) carrying out experiments statistically designed according to the experimental design, (2) proposing the mathematical model based on the experimental results and working out the result of the analysis of variance, and (3) predicting the response and confirming the model. The experimental results are shown in Table 5.

The empirical mathematical model (equation (4)) was used to evaluate the correlation between the experimental values and the predicted values. These quadratic model equations represent the fit between the predicted responses and the four coded variables: the initial concentration (A), the pH of the solution (B), the contact time (C), and the mass of the carbon (D). We denote by Y_{HQ} and Y_R, respectively, the responses which are the adsorbed quantities of hydroquinone and resorcinol by CAK-S.

$$\begin{aligned} Y_{HQ} = {} & 13.2253 + 0.5210A - 1.63672B - 0.10589C \\ & - 0.06754\ D - 0.00154A^2 - 0.00573\mathrm{AB} + 0.000002\mathrm{AC} \\ & - 0.00042\mathrm{AD} + 0.15385B^2 - 0.00254\mathrm{BC} \\ & + 0.00007\mathrm{BD} + 0.00091C^2 - 0.00012\mathrm{CD} + 0.00009D^2, \end{aligned} \tag{5}$$

$$\begin{aligned} Y_R = {} & 7.3315 + 0.18979A - 3.19280B + 0.04996C \\ & + 0.15455\ D - 0.00029A^2 - 0.01179\mathrm{AB} + 0.00002\mathrm{AC} \\ & + 0.00001\mathrm{AD} + 0.27958B^2 - 0.00944\mathrm{BC} \\ & + 0.00388\mathrm{BD} - 0.00031C^2 + 0.00015\mathrm{CD} - 0.00076D^2. \end{aligned} \tag{6}$$

These equations with positive and negative coefficients can be used to illustrate optimal results.

Analysis of variance (ANOVA) was used to identify the relationships between the different variables on the quantities adsorbed (Table 6). A factor is said to be significant when, at the 95% confidence interval, the probability value (p value) is less than 5% and R^2 is close to unity. With regard to the adsorption of hydroquinone onto CAK-S, the individual variables A, B, and D as well as the interactions AA, AB, and AD have a significant influence on the quantity adsorbed. For the adsorption of resorcinol, factors A, B, C, and D and the interactions AB and DD significantly influence its quantity adsorbed. By eliminating statistically insignificant terms, the quadratic models reduce to equations (7) and (8). These reductions can be translated into response surfaces in order to identify areas of interest and therefore determine optimal conditions

Table 3: Nonlinear forms of kinetic and isotherms models.

Models	Nonlinear forms	References
	Kinetic models	
Pseudo-first-order	$q_t = q_e(1 - e^{-k_1 t})$	[31]
Pseudo-second-order	$q_t = k_2 q_e^2 t/1 + k_2 q_e t$	[32]
Elovich	$q_t = \ln(\alpha\beta)/\beta + \ln(t)/\beta$	[33]
Interparticle diffusion	$q_t = K_{i\,d} t^{1/2} + C$	[34]
	Two-parameter isotherms	
Langmuir	$Q_e = Q_m K_L C_e/1 + K_L C_e$	[35]
Freundlich	$Q_e = K_F \mathrm{Ce}^{1/n}$	[35]
Dubinin–Radushkevich	$Q_e = Q_m \exp(-K'\varepsilon^2)$, $\varepsilon = \mathrm{RTLn}(1 + 1/C_e)$, $E = (2K_D)^{-1/2}$	[36]
Temken	$Q_e = \mathrm{RT}/\Delta Q \ln(A_T C_e)$	[37]
	Three-parameter isotherms	
Redlich-Peterson	$Q_e = \mathrm{AC}_e/1 + \mathrm{BC}_e^{\beta}$	[38]
Sips	$Q_e = K_s C_e^{\beta}/1 + a_s C_e^{\beta s}$	[38]
Toth	$Q_e = Q_m C_e/(K_T + C_e^n)^{1/n}$	[39]
Hill	$Q_e = Q_{\mathrm{SH}} C_e^{\mathrm{nH}}/K_D + C_e^{\mathrm{nH}}$	[39]
Kahn	$Q_e = Q_{\max} b_K C_e/(1 + b_K C_e) a_k$	[39]

Table 4: Error functions and their equations.

Error function	Abbreviation	Formula	References
Residual root mean square error	RMSE	$\sqrt{(1/n - 1\sum_{i=1}^{n}(q_{e,\exp} - q_{e,\mathrm{cal}}))^2}$	[42]
Average ralative error	ARE	$100/n\sum_{i=1}^{n}\lvert q_{e,\exp} - q_{e,cal}/q_{e,\exp}\rvert_i$	[43]
Sum of absolute errors	EABS	$\sum_{i=1}^{n}\lvert q_{e,\exp,i} - q_{e,\mathrm{cal},i}\rvert$	[42]
Hybrid fractional error function	HYBRID	$100/n - p\sum_{i=1}^{n}[(q_{e,\exp} - q_{e,\mathrm{cal}})/q_{e,\exp}]$	[38]
Nonlinear chi-square test	χ^2	$\sum_{i=1}^{n}(q_{e,\mathrm{cal}} - q_{e,\exp})/q_{e,\exp}^2$	[44]
Coefficient of determination	R^2	$(q_{e,\exp} - \overline{q_{e,\mathrm{cal}}})/\sum(q_{e,\exp} - \overline{q_{e,\mathrm{cal}}}) + (q_{e,\exp} - q_{e,\mathrm{cal}})$	[43]

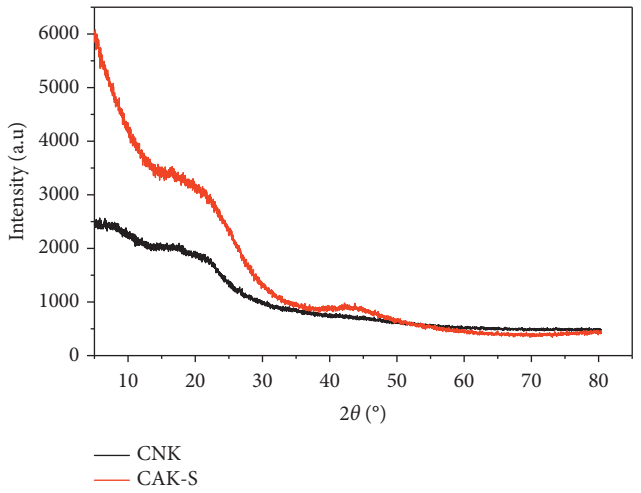

Figure 1: Superimposed XRD spectra of CNK shea nut shells and CAK-S activated carbon.

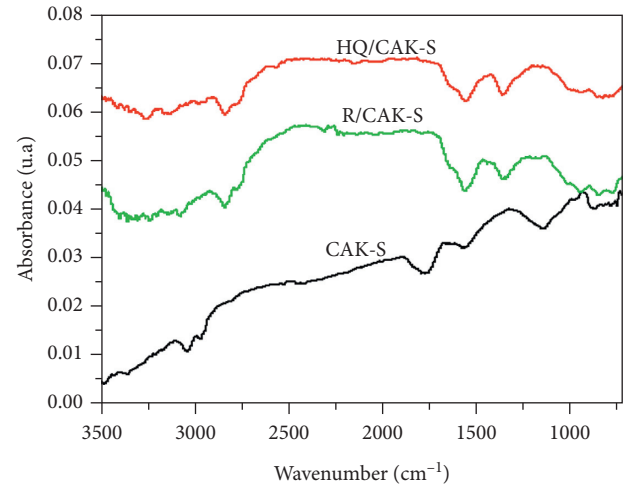

Figure 2: FTIR spectrum of CAK-S before and after adsorption of HQ and R.

$$Y'_{\mathrm{HQ}} = 13.2253 + 0.5210A - 1.63672B - 0.06754\ D - 0.00154A^2 - 0.00573\mathrm{AB} - 0.00042\mathrm{AD}, \quad (7)$$

$$Y'_R = 7.3315 + 0.18979A - 3.19280B + 0.04996C + 0.15455\ D - 0.01179\mathrm{AB} - 0.00076D^2. \quad (8)$$

3.3. Interactions of Independent Variables. The three-dimensional response surface curves are plotted only for the most important factor interactions. In Table 6, we see at 5% the most important interactions between concentration and pH with a probability $P = 0.0021$ and then concentration and mass with $P = 0.0000$. These interactions are shown in Figure 3. An increase in the quantity of HQ adsorbed is

Table 5: Matrix of coded variables associated with experimental and predicted values of adsorption of hydroquinone or resorcinol on CAK-S.

Adsorption of hydroquinone (HQ) or resorcinol (R) on activated carbon CAK-S										
No.	Coded levels				HQ			R		
	A	*B*	*C*	*D*	Exp qads	Prev qads	Residu	Qads exp	Qads prev	Residu
1	0	−1	0	0	24.12	27.17	−3.05	21.27	25.64	−4.37
2	−1	0	0	0	5.37	3.42	5.34	4.21	9.55	−5.34
3	+1	−1	+1	−1	45.11	44.28	0.83	33.58	29.49	4.09
4	−1	+1	+1	+1	2.37	1.56	0.81	2.13	0.21	1.92
5	0	0	0	0	23.82	22.52	1.30	16.44	16.60	−0.16
6	0	+1	0	0	24.82	22.81	2.01	20.90	16.50	4.40
7	0	0	0	0	23.91	22.52	1.39	17.14	16.60	0.54
8	0	0	0	+1	14.38	14.39	−0.01	5.65	5.17	0.48
9	−1	−1	+1	+1	3.03	3.09	−0.06	2.67	2.08	0.59
10	+1	+1	+1	−1	36.66	35.29	1.37	2.27	6.29	−4.02
11	−1	−1	−1	−1	15.17	13.88	1.29	12.74	12.38	0.36
12	+1	+1	−1	+1	13.00	14.06	−1.06	5.11	7.84	−2.73
13	0	0	0	−1	31.48	32.48	−1.00	12.31	12.76	−0.45
14	+1	0	0	0	18.85	21.76	−2.91	25.27	19.91	5.36
15	0	0	+1	0	23.75	24.21	−0.46	10.80	14.67	−3.87
16	−1	−1	−1	+1	3.04	3.54	−0.50	2.66	0.05	2.61
17	+1	+1	+1	+1	7.58	9.47	−1.89	4.51	3.45	1.06
18	+1	−1	−1	−1	42.62	42.56	0.06	26.53	29.86	−3.33
19	−1	+1	+1	−1	12.61	13.92	−1.31	4.33	3.54	0.79
20	−1	+1	−1	+1	2.41	3.84	−1.43	2.30	4.97	−2.67
21	0	0	0	0	22.08	22.52	−0.44	16.74	16.60	0.14
22	+1	−1	−1	+1	19.46	18.75	0.71	18.65	18.03	0.62
23	+1	+1	−1	−1	34.87	35.41	0.54	14.30	13.47	0.83
24	−1	+1	−1	−1	13.80	11.73	2.07	11.53	11.08	0.45
25	0	0	0	0	23.31	22.52	0.79	16.02	16.60	−0.58
26	−1	−1	+1	−1	15.17	13.88	1.29	12.97	11.65	1.32
27	+1	−1	+1	+1	19.46	18.33	1.13	18.57	20.43	−1.86
28	0	0	−1	0	23.93	24.49	−0.56	21.14	17.24	3.90

A: initial concentration (mg/L) of hydroquinone or resorcinol, *B*: pH of solution, *C*: contact time (min), and *D*: mass of activated carbon (mg).

Table 6: Analysis of variance (ANOVA) of adsorbed quantity of hydroquinone and resorcinol by CAK-S.

		Hydroquinone				Resorcinol			
Source	Df	SS	MC	*F* value	*p* value	SS	MC	*F* value	*p* value
A	1	1509.91	1509.91	410.49	0.0000*	385.03	385.03	31.83	0.0001*
B	1	84.76	84.76	23.10	0.0003*	290.08	290.08	23.98	0.0003*
C	1	0.30	0.36	0.10	0.7577	60.97	60.97	05.04	0.0428*
D	1	1471.71	1471.71	401.17	0.0000*	188.89	18889	15.62	0.0017*
A^2	1	252.72	252.72	68.89	0.0000*	10.87	10.87	0.90	0.3604
AB	1	53.73	53.73	14.05	0.0021*	158.69	158.69	13.12	0.0031*
AC	1	0.01	0.01	0.00	0.9800	4.55	4.55	038	0.5504
AD	1	181.31	181.31	49.42	0.0000*	8.95	8.95	0.74	0.4051
B^2	1	15.63	15.63	4.26	0.0595	47.52	47.52	3.93	0.0690
BC	1	3.36	3.36	0.92	0.3555	18.51	18.51	1.53	0.2379
BD	1	0.02	0.02	0.00	0.9400	13.86	13.86	1.15	0.3040
C^2	1	8.65	8.65	2.36	0.1485	1.75	1.75	0.14	0.7101
CD	1	4.57	4.57	1.25	0.2841	27.85	27.85	2.30	0.1531
D^2	1	2.19	2.19	0.60	0.4534	157.45	157.45	13.02	0.0032*
		$R^2 = 98.69\%$, adjusted $R^2 = 97.29\%$				$R^2 = 90.55\%$, adjusted $R^2 = 80.38\%$			

*Significant. D: degree of freedom; SS: sum of squares; MS: mean square; adjusted R^2: adjusted R^2.

observed as a function of the increase in initial concentration. This is due to the increase in HQ molecules in the solution creating competition for different adsorption sites. The opposite is observed with increasing pH. In fact, the adsorption capacity of CAK-S decreases as the pH increases (Figure 3(a)). For pH > 6.37 (pHpzc), the carbon surface is negatively charged, and, for values of pH > 8, HQ in turn loses its protons and becomes a monoanion hydroquinate ($HQ(OH)(O)^-$) or a dianion hydroquinate ($HQ(O)2^-$) [1]. The repulsion between the negatively charged CAK-S

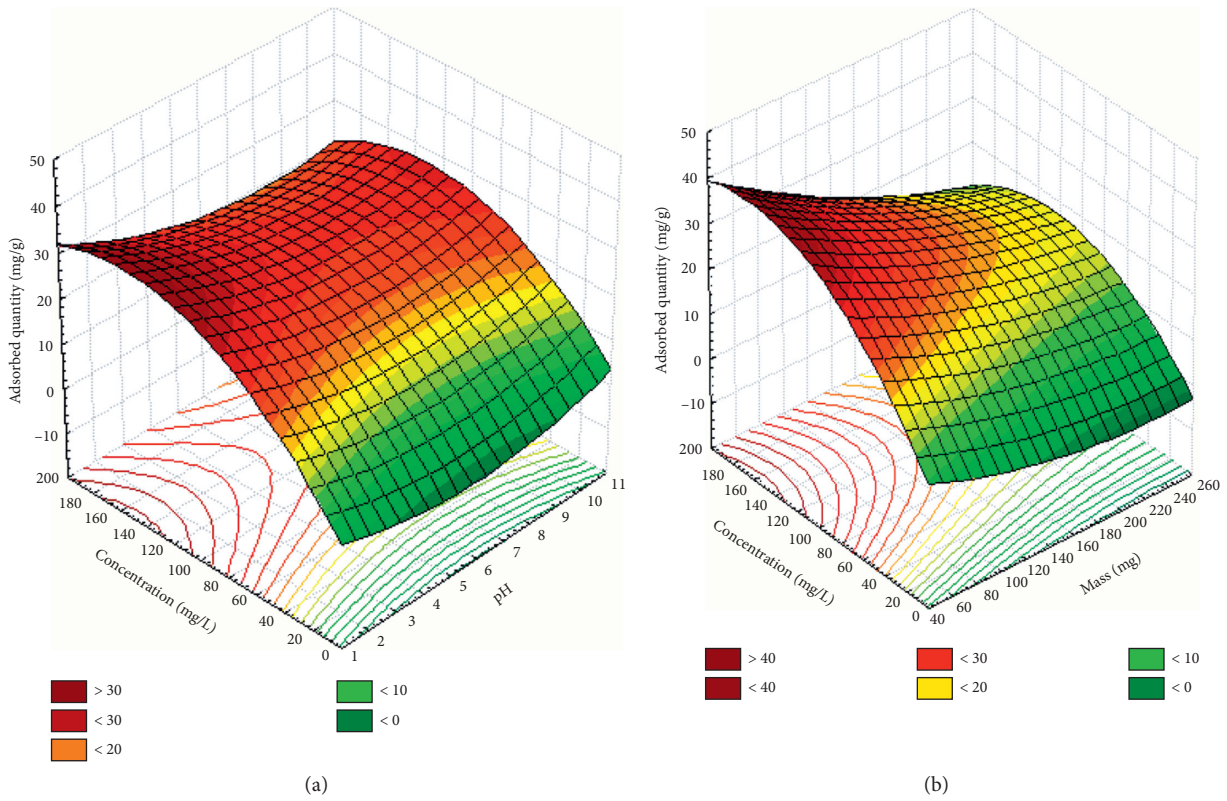

Figure 3: 3D surface plot of the adsorbed quantities of HQ by CAK-S as a function of (a) concentration and pH and (b) concentration and mass.

surface layer and the hydroquinate anion results in a considerable decrease in the quantity of HQ adsorbed. For this study, statistical analysis showed that the synergistic effect of concentration and the antagonistic effect of pH at high values lead to maximum adsorption at pH 3. At this pH, the surface area of CAK-S is charged with protons and HQ is stable in acidic conditions. Adsorption is maximum on the one hand by formation of hydrogen bonds with the hydroxyl groups and, on the other hand, by π-π interactions of benzene rings between HQ and CAK-S [17, 45]. In Figure 3(b), we see a decrease in the quantity of HQ adsorbed with increasing mass. This is explained by the formation of CAK-S particle clusters inducing a reduction in the total adsorption surface area and therefore a decrease in the amount of adsorbate per unit mass [46].

Regarding the adsorption of R by CAK-S, only the interaction between concentration and pH with a probability $P = 0.0031$ is significant. Figure 4 shows the 3D visualization of this interaction. It appears that the amount of R adsorbed increases as the initial concentration increases, which is also explained by a large number of R molecules in solution. The adsorbed amount of R decreases as the pH increases. This is justified by the fact that, at pH $>$ pKa, a repulsion is created between the resorcinolate anions ($R(OH)(O)^-$ or $R(O)2^-$) and the negatively charged CAK-S surface. In the region of pH $<$ 6.37 (pHpzc), the surface of CAK-S is positively charged and there is formation of hydrogen bonds and π-π attraction interactions between the molecules of R and those of the surface of CAK-S.

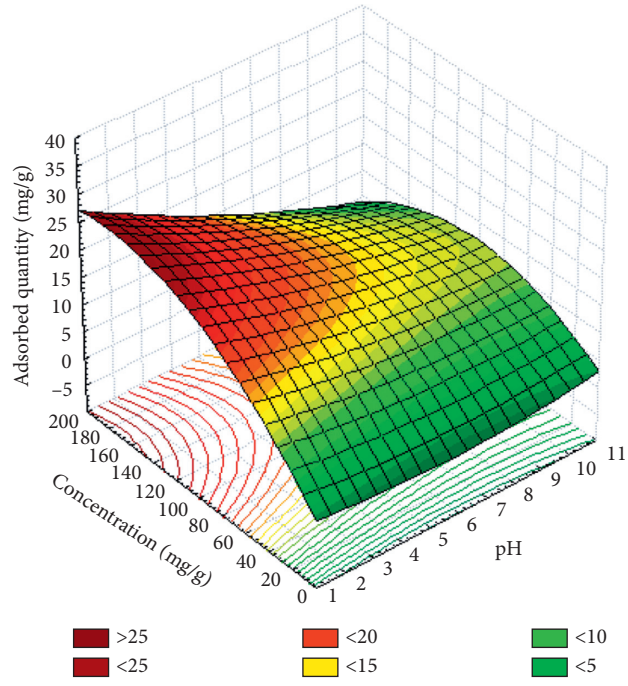

Figure 4: 3D surface graph of the adsorbed quantities of R by CAK-S as a function of concentration and pH.

3.4. Process Optimization and Test Validation. The optimal conditions for binding of HQ and R to CAK-S (Table 7) result from a statistical analysis of the experimental data by

Table 7: Validation of the experimental model of the adsorption of HQ and R by CAK-S.

Adsorbates	Operational variables		Adsorbed quantity (mg/g) Exp. val.	Pred. val.	Residue
HQ	*A* (mg/L)	158	45.02	45.66	−0.64
	B	3			
	C (min)	120			
	D (mg)	50			
R	*A* (mg/L)	180	33.65	32.67	0.98
	B	3			
	C (min)	86			
	D (mg)	118			

STATGRAPHIC Plus 5.0 software. A new HQ and R adsorption experiment was repeated to confirm the best level obtained for each operating variable leading to the optimal predicted results. It emerges from this experiment that the difference between the experimental and predicted values is small, and this demonstrates the validity of the model. Therefore the experimental data are satisfactory and agree with the studied model. These results complete the analysis of variance (Table 6) which presents the high values of the correlation coefficients ($R^2 > 90$) and the adjusted correlation coefficients (adjusted $R^2 > 80$).

3.5. Nonlinear Adsorption Kinetic Studies. In order to elucidate the sorption mechanism of hydroquinone or resorcinol on CAK-S activated carbon, the contact time was varied between 5 and 160 min. The other parameters were set at their optimum values. Kinetic models such as the pseudo-first-order, pseudo-second-order, Elovich, and intraparticle diffusion models were investigated. The nonlinear plots are shown in Figures 5 and 6. Table 8 shows the calculated values of all parameters. It emerges that the nonlinear kinetic pseudo-first-order, pseudo-second-order, and Elovich models are more appropriate for the description of the adsorption of HQ and R on the CAK-S, because the coefficients of determination are closer to unity ($R^2 > 0.99$). However, the low value of χ^2 and the low values of the error functions obtained from the Elovich model show that it is the best kinetic model to describe the adsorption of HQ and R. This model suggests that the adsorption of HQ or R is primarily chemical and the active sites on the surface of CAK-S are heterogeneous [25]. This is confirmed by the values of the desorption constant $\beta < 1$ (0.198 and 0.313 mg/g.min, respectively, for HQ and R). Observation of the pseudo-first-order kinetic model (Figures 4 and 5) shows that the binding of HQ or R molecules to the surface of CAK-S occurs rapidly, thereby reaching equilibrium. For pseudo-second-order kinetics, the amounts adsorbed at equilibrium are close to experimental ones, which demonstrates the existence of majority π-π type interactions [47].

3.6. Modeling of Nonlinear Adsorption Isotherm. To model the adsorption isotherms with the experimental data, the effect of initial concentrations of HQ and R was studied in the range of 40 to 180 mg/L using optimal conditions. The equilibrium results were modeled with four two-parameter models and five

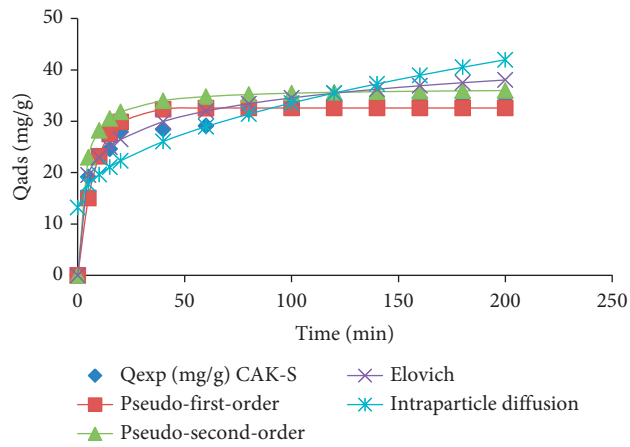

Figure 5: Nonlinear plot of kinetic models of HQ adsorption by CAK-S.

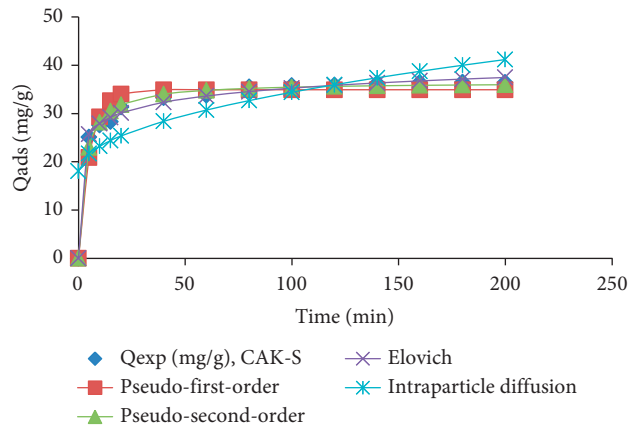

Figure 6: Nonlinear plot of kinetic models of R adsorption by CAK-S.

three-parameter models. Two-parameter adsorption isothermal equilibrium simulations of the two-parameter adsorption isotherms of HQ and R by CAK-S are shown in Figures 7 and 8. All calculated parameters are shown in Table 9.

It emerges from this table that the values of coefficients of determination, R^2, are close to unity for the Langmuir, Freundlich, and Temkin models. These models can be exploited to explain the adsorption of HQ and R. Based on the high value of R^2, low value of χ^2, and low values of the RMSE, HYBRID, ARE, and EABS error functions, Temkin

Table 8: Kinetic data obtained by nonlinear fitting analysis (see equations in Table 3 and 4).

Models	Parameters		R^2	χ^2	Errors RMSE	HYBRID	ARE	EABS
			HQ/CAK-S					
Pseudo-first-order	q_e (mg/g) K_1 (1/min)	32.577 0.124	0.994	0.189	2.479	1.575	0.028	1.577
Pseudo-second-order	q_e (mg/g) K_2 (g/min.mg)	37.164 0.004	0.991	0.258	2.962	2.151	0.027	1.558
Elovich	A (mg/g.min) B (mg/g.min)	47.579 0.198	0.998	0.072	1.562	0.597	0.001	0.042
Intraparticle diffusion	K_{id} (mg/g.min$^{0.5}$) C (mg/g)	2.036 13.182	0.979	0.658	4.732	5.488	3.5×10^{-6}	0.000
			R/CAK-S					
Pseudo-first-order	q_e (mg/g) K_1 (1/min)	34.930 0.182	0.996	0.143	2.269	1.191	0.017	1.057
Pseudo-second-order	q_e (mg/g) K_2 (g/min.mg)	36.503 0.009	0.998	0.030	1.045	0.253	0.003	0.187
Elovich	A (mg/g.min) B (mg/g.min)	2007.7 0.313	0.999	0.014	0.723	0.121	2.33×10^{-5}	0.001
Intraparticle diffusion	K_{id} (mg/g.min$^{0.5}$) C (mg/g)	1.636 18.048	0.967	1.135	6.396	9.453	5.02×10^{-7}	3.04×10^{-5}

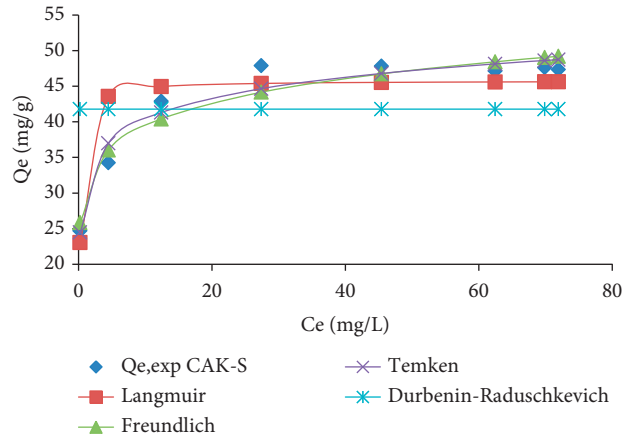

Figure 7: Nonlinear plot of two-parameter adsorption isotherm models of HQ by CAK-S.

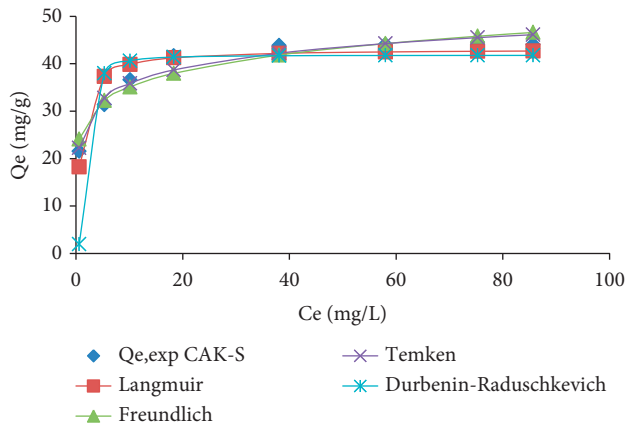

Figure 8: Nonlinear plot of two-parameter adsorption isotherm models of R by CAK-S.

model is found to better describe the adsorption isotherm of HQ and R by the activated carbon CAK-S. This Temkin model highlights a decrease in interactions between HQ or R molecules followed by a linear decrease in heat of adsorption with surface coverage. The adsorption energies of this model are positive (587.068 and 514.132 J/mol, respectively, for HQ and R); this is evidence of chemisorption and the process is exothermic [26]. Given the values of R^2 and those of χ^2, the Langmuir isotherm can describe the adsorption of the two pollutants. It suggests a monolayer adsorption on the surface of the carbon, without interaction between the adsorbed molecules. By comparing the maximum adsorption capacity Q_m (Table 9), we find that hydroquinone is more adsorbed: 45.764 mg/g against 43.097 mg/g for resorcinol. Patricia et al. [3] obtained similar results. This is due to the solubility and configuration of these isomers. This is because resorcinol is more soluble than hydroquinone in water. The more soluble a substance is, the less it is adsorbed. The paraposition and metaposition of hydroxyl groups on benzene also influence adsorption. Indeed, according to the 1–4 position of hydroxy groups on benzene, hydroquinone is a symmetrical and stable molecule. This configuration allows it to easily access adsorption sites due to its greater energy stability [3]. Freundlich model's n values greater than 1 showed good affinity of the adsorbates with the material and the adsorption process occurred on heterogeneous surfaces, characterizing adsorption at localized sites [35, 48]. In short, the modeling of two-parameter isotherms leans towards the adsorption of HQ or R taking place on a heterogeneous surface with a nonuniform absorption energy distribution.

3.6.1. Three-Parameter Adsorption Isothermal Equilibrium. The nonlinear plots of the isothermal models with three parameters studied are presented in Figures 9 and 10. Table 10 gives the values of constants related to these nonlinear regression isotherm models.

Table 9: Adsorption of hydroquinone and resorcinol: nonlinear fitting analysis for two-parameter isotherms (see equations in Tables 3 and 4).

Models	Parameters		R^2	χ^2	Errors			
					RMSE	HYBRID	ARE	EABS
			HQ/CAK-S					
Langmuir	Q_m (mg/g)	45.764	0.992	0.336	4.363	5.603	0.014	0.385
	K_L (L/min)	4.424						
Freundlich	K_F (mg/L)	30.482	0.997	0.096	2.335	1.605	0.162	0.005
	n	8.930						
Temken	A_T (L/mg)	1430.831	0.998	0.074	2.054	1.243	0.0006	2.52×10^{-6}
	ΔQ (J/mol)	587.068						
Dubinin-Radushkevich	Q_m (mg/g)	41.783	0.957	1.522	9.283	25.368	5.443	0.200
	K_{id} (L/mg)	5.12×10^{-7}						
	E (kJ/mol) = 988.21							
			R/CAK-S					
Langmuir	Q_m (mg/g)	43.097	0.994	0.222	3.371	3.695	0.040	0.986
	K_L (L/min)	1.212						
Freundlich	K_F (mg/L)	25.795	0.997	0.116	2.436	1.929	0.283	0.011
	n	7.524						
Temken	A_T (L/mg)	166.865	0.998	0.064	1.818	1.074	0.0001	7.35×10^{-6}
	ΔQ (J/mol)	514.132						
Dubinin-Radushkevich	Q_m (mg/g)	41.783	0.964	1.522	8.835	25.372	18.758	0.762
	K_{id} (L/mg)	5.26×10^{-7}						
	E (kJ/mol) = 974.97							

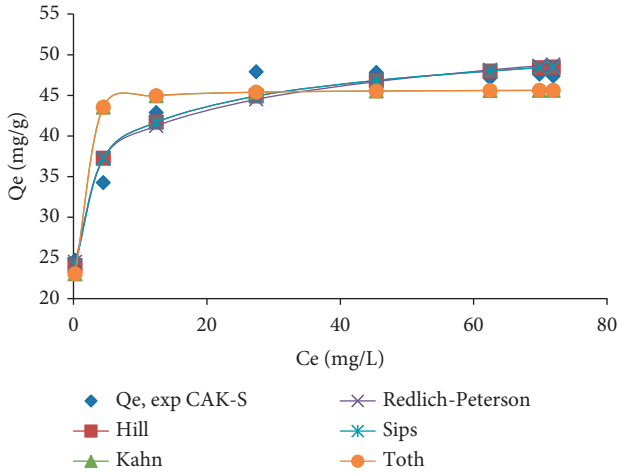

Figure 9: Nonlinear plot of three-parameter adsorption isotherm models of HQ by CAK-S.

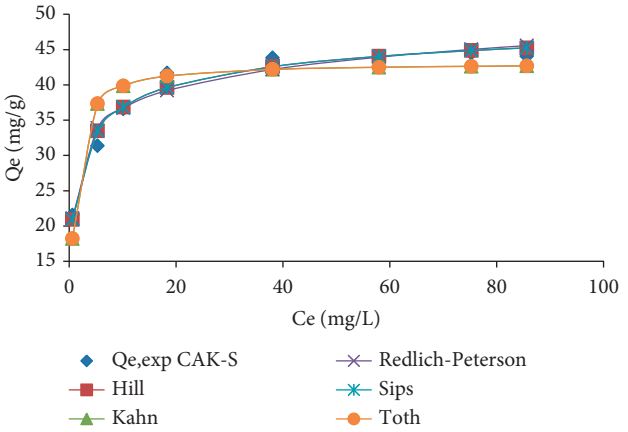

Figure 10: Nonlinear plot of three-parameter adsorption isotherm models of R by CAK-S.

We notice in Table 9 that the values of the coefficient of determination R^2 for all the isotherm models are close to unity ($R^2 > 0.99$) and the values of the corresponding error functions are low, which suggest that these models are suitable for effectively describing experimental data at equilibrium. The Sips model, having the high values of R^2 and the low values of χ^2, shows a distribution of the molecules of HQ and of R on a heterogeneous surface of CAK-S, thus presenting energetically different adsorption sites [49]. The values of the constant n_H of the Hill model different from 1 highlight a localized adsorption [38] with formation of a bond between the molecules of HQ or R and that of carbon. The values of the β heterogeneity parameter of the Redlich-Peterson model between 0 and 1 show that the model cannot be reduced to a single-layer adsorption but rather to a so-called heterogeneous system. These results confirm those of the two-parameter models which suggest that the adsorption of HQ or R occurs on heterogeneous surfaces of CAK-S, with a nonuniform adsorption energy distribution.

3.7. Effect of Temperature and Thermodynamics of Adsorption. The thermodynamic study was carried out by varying the temperature by 30, 40, 50, 60, and 70°C. The tests were carried out with 30 mL of solution and using the optimum conditions required for the adsorption of each pollutant by CAK-S. Thermodynamic parameters such as Gibbs standard free energy (ΔG^0), standard enthalpy (ΔH^0), and standard entropy (ΔS^0) are related by the two following equations [22]:

Table 10: Adsorption of hydroquinone and resorcinol: nonlinear fitting analysis for three-parameter isotherms (see equations in Tables 3 and 4).

Models	Parameters		R^2	χ^2	Errors			
					RMSE	HYBRID	ARE	EABS
			HQ/CAK-S					
	Q_m (mg/g)	65.611						
Hill	K_H (L/g)	0.276	0.998	0.068	1.967	1.368	0.002	0.045
	n_H	1.150						
	Q_{max} (mg/g)	69,940						
Kahn	b_K (L/g)	4.424	0.992	0.336	4.363	6.723	0.014	0.385
	a_K	1.528						
	A (L/g)	757.85						
Redlich-Peterson	B (L/mg)	23.149	0.998	0.083	2.168	1.661	0.0018	0.022
	β	0.905						
	K_S (L/g)	57.005						
Sips	a_S (L/g)	0.868	0.998	0.068	1.967	1.368	0.002	0.046
	β_S	0.276						
	Q (mg/g)	45.764						
Toth	K_e	0.832	0.992	0.336	4.363	6.723	0.014	0.385
	N	0.120						
			R/CAK-S					
	Q_m (mg/g)	52.907						
Hill	K_H (L/g)	0.443	0.998	0.040	1.434	0.802	0.002	0.060
	n_H	1.220						
	Q_{max} (mg/g)	92.049						
Kahn	b_K (L/g)	1.212	0.994	0.222	3.372	4.435	0.040	0.986
	a_K	2.135						
	A (L/g)	123.84						
Redlich-Peterson	B (L/mg)	4.026	0.998	0.058	1.372	1.177	0.001	0.032
	β	0.911						
	K_S (L/g)	43.344						
Sips	a_S (L/g)	0.819	0.998	0.040	1.436	0.803	0.002	0.060
	β_S	0.444						
	Q (mg/g)	43.097						
Toth	K_e	0.976	0.994	0.222	3.372	4.436	0.040	0.986
	N	0.126						

$$\Delta G^0 = -\mathrm{RT} \ln K_d, \tag{9}$$

$$\ln K_d = \left(\frac{\Delta S^0}{R}\right) - \left(\frac{\Delta H^0}{R}\right)\frac{1}{T}. \tag{10}$$

We have that $K_d = 1000\ Q_e/C_e$ is the distribution constant, Q_e (mg/g) is the adsorbed quantity of pollutant at equilibrium, C_e (mg/L) is the residual concentration of the target compound in solution, R (8.314 J/mol.K) is the constant of ideal gases, and T (K) is the absolute temperature. The results are shown in Figure 11.

Figure 11(a) shows the influence of temperature on the retention of HQ or R. It appears that the adsorbed quantity increases with increasing temperature, suggesting that the process is endothermic, and that the increase in temperature promotes the progression of adsorption. Table 11 summarizes the values of ΔG^0, ΔH^0, and ΔS^0 obtained from extrapolation of the linear plot $\ln K_d = f(1/T)$ (Figure 11(b)). The less negative values of ΔG^0 with increasing temperature show that the adsorption of HQ or R by CAK-S is favorable and spontaneous. Positive values of ΔH^0 indicate an endothermic nature of the adsorption process. These low positive values of enthalpy ($\Delta H^0 < 40$ kJ/mol) are characteristics of a physisorption. Positive entropy values ΔS^0 also indicate increased randomness, including the number of species at the solid-liquid interface during sorption. Similar results were obtained during adsorption of hydroquinone in solution by granular activated carbon [1] and adsorption of hydroquinone by hydroxyethyl cellulose functionalized with magnetic/ionic liquid [49].

3.8. Mechanism Involving Hydrogen Bonding and π-π and n-π Interactions. The binding mechanism of HQ and R is discussed on the basis of surface properties of CAK-S and modeling results. In general, the surfaces of activated carbons are made of acid functions like carboxyl, hydroxyl, quinones, carbonyl, and lactone groups, as well as basic functions like pyrones and chromenes [4, 50, 51]. For the case of CAK-S, the FTIR and the Boehm titration results, supplemented by EDX/SEM [28], have shown that it has the chemical functions mentioned above. These functional groups act as nucleophilic and electrophilic sites likely to react with the hydroxyl groups and the delocalized π electron system of the benzene ring present in HQ or R. The results of the thermodynamic study show that the adsorption was mainly dominated by physisorption ($\Delta H^0 < 40$ kJ/mol).

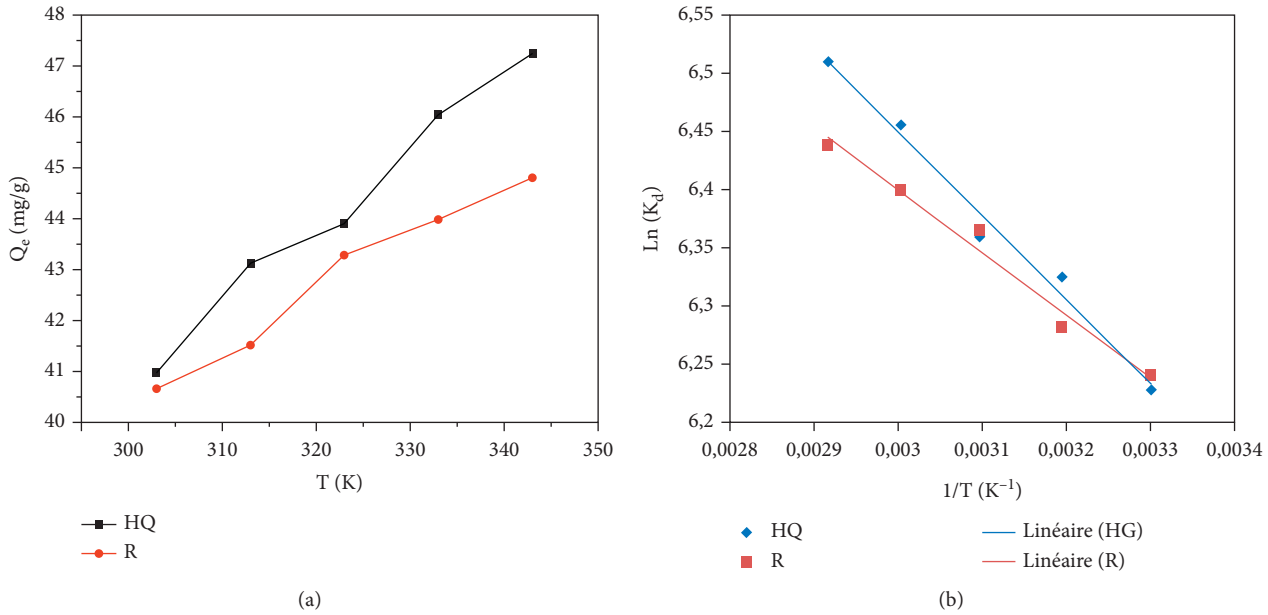

Figure 11: (a) Effect of temperature. (b) Linear plot ln (Kd) versus 1/T of the adsorption of HQ or R.

Table 11: Thermodynamics parameters of the adsorption of HQ and R.

Temperature (K)	HQ			R		
	ΔG^0 (kJ/mol)	ΔH^0 (kJ/mol)	ΔS^0 (J/mol.K)	ΔG^0 (kJ/mol)	ΔH^0 (kJ/mol)	ΔS^0 (J/mol.K)
303	−15.871			−15.719		
313	−16.446			−16.342		
323	−17.080	5.992	71.59	−17.079	4.447	66.54
333	−17.857			17.691		
343	−18.565			18.364		

However, Temkin model with positive adsorption energy (587.068 and 514.132 J/mol, respectively, for HQ and R) suggests chemisorption, but this was fairly minimal and was not a control mechanism. Likewise, FTIR analysis reveals shifts in the absorption bands of functional groups (hydroxyl, carboxylate, and C–O) after adsorption of HQ and R by CAK-S, but these were also small for controlling the process. For an optimal value of pH = 3 (lower than pHpzc 6.37), the carbon surface is positively charged and easily attracts electrons from HQ and R. In addition, the hydroxyl, carboxylate, and C–O functional groups on the surface of CAK-S are rich in oxygen atoms (electronegative atom), which is a good candidate for physical interactions. The main physical adsorption mechanisms involved are based on the Van der Waals forces of attraction, in particular the hydrogen bonds which are likely to play a role in absorption [52]. Based on this observation, we see that there is a coexistence of chemisorption and physisorption, with the latter being dominant during sorption of HQ or R on CAK-S. In the end, the two aromatic isomers have hydroxyl groups which largely participate in the binding onto CAK-S, consequently supported by π-π and n-π interactions as well as the formation of hydrogen and covalent bonds. It should be noted that the attachment of these isomers to CAK-S also depends on the paraposition and metaposition of the hydroxyl groups. The HQ in hydroxide position 1–4 on benzene is symmetrical and stable and therefore is easily accessible at binding sites due to its greater energy stability, compared to R in the metaposition [3]. For this reason, we have chosen to represent only (Figure 12) the binding mechanism of hydroquinone, which has a high affinity with CAK-S activated carbon. The mechanism by which resorcinol binds to this AC is similar to that of hydroquinone.

3.9. Comparison with Other Adsorbents. The adsorption efficiency of HQ and R in aqueous solution using various adsorbents is shown in Table 12. It appears that CAK-S is shown to be a capable adsorbent that can be exploited in the removal of HQ and R of wastewater compared to other adsorbent materials. Although the operating conditions are not the same, CAK-S exhibits higher maximum removal efficiency than some adsorbents reported in previous studies. These results contribute to environmental remediation because CAK-S produced from local biomass can be exploited specifically for effective attenuation of HQ and R in aqueous media.

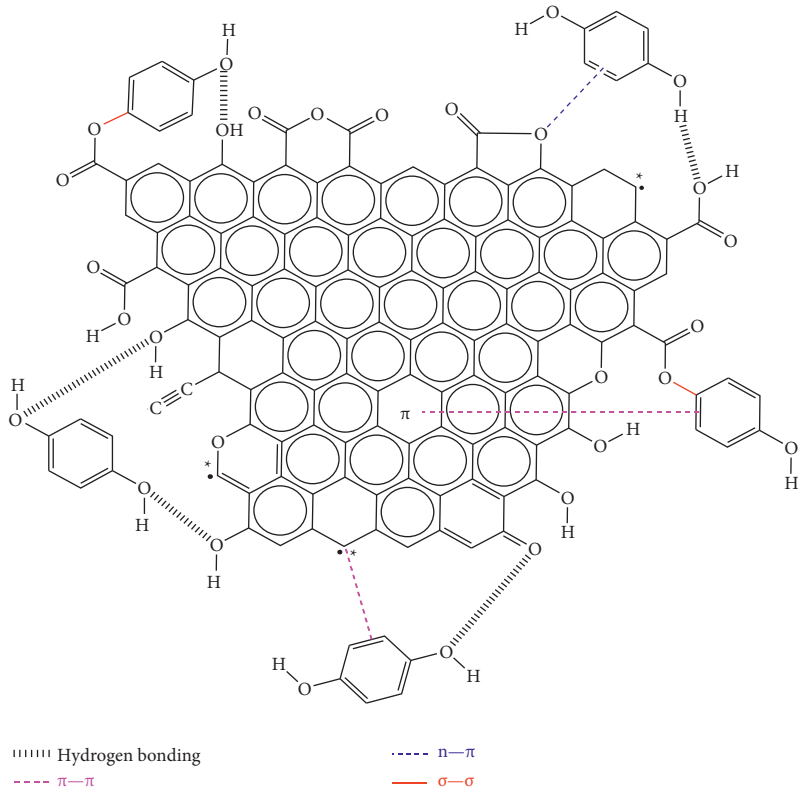

Figure 12: Possible interactions contributing to the mechanism of hydroquinone adsorption on CAK-S except pore filling.

Table 12: Comparison of CAK-S with other materials for HQ and R reduction.

Adsorbent	Condition	Adsorbed quantity	References
	Adsorption of hydroquinone by some adsorbents		
CAK-S	$C = 158$ mg/L; pH = 3; $t = 120$ min; $m = 50$ mg	45.02 mg/g	Present study
Activated carbon based on monkey kola (*Cola lepidota* K. Schum) waste	$C = 55.55$ mg/L; pH = 6; $t = 30$ min; $m = 100$ mg	7.33 mg/g (66.57 μmol/g)	[3]
Iron impregnated granular activated carbon	$C = 100$ mg/L, pH = 4, $t = 14$ h, m = 40 g/L	26.55 mg/g	[53]
	Adsorption of resorcinol by some adsorbents		
CAK-S	$C = 180$ mg/L; pH = 3; $t = 86$ min; $m = 118$ mg	33.65 mg/g	Present study
Activated carbon based on monkey kola (*Cola lepidota* K. Schum) waste	$C = 55.55$ mg/L; pH = 6; $t = 30$ min; $m = 100$ mg	0.60 mg/g (5.47 μmol/g)	[3]
OMC	$C = 20$ mg/L; pH = 6.5; $t = 24$ h; $m = 0.1$ g/L	34.4 mg/g	[54]

4. Conclusion

The response surface methodology was used as a simple approach to optimize the binding of HQ and R in solution on activated carbon from shea residue. The study focused on the main factors (concentration of target pollutants, pH of the solution, contact time, and mass of carbon) having an effect on the quantity adsorbed. The optimal conditions obtained from the statistical analysis were concentration of 158 mg/L, pH 3, mass of 50 mg, and time of 120 min for the HQ and a concentration of 180 mg/L, pH 3, time of 86 min, and mass of 118 mg for R. For these conditions, the maximum quantities of HQ and R adsorbed are 45.02 and 33.65 mg/g, respectively. The adsorption was better described using Elovich kinetics which suggest that the CAK-S surface is heterogeneous. Also, the Temkin two-parameter and the Sips three-parameter isotherm models suggest a heterogeneous surface with a nonuniform adsorption distribution energy. The process was spontaneous ($-\Delta G^0$) and endothermic ($+\Delta H^0$) and resulted in increased disorder of species in solution ($+\Delta S^0$). The π-π, n-π interactions, hydrogen bonds, and pores filling were the main contributors to the mechanism of binding of HQ and R to CAK-S. This CAK-S material has shown good HQ and R removal performance, which is a very significant contribution to environmental remediation. It can be exploited specifically by environmentalists for effective mitigation of phenolic compounds from wastewater.

Data Availability

The digital data used to support the conclusions of this study have been deposited in the Mendeley repository

(http://www.mendeley.com/reference-manager/library/recently-read).

Conflicts of Interest

The authors declare that they have no conflicts of interest.

Acknowledgments

The authors appreciate the technical assistance of the Researchers of Material and Process Engineering Team (MPET)/RU-NOCHEE of the Department of Chemistry, Faculty of Science, University of Dschang, Cameroon. The authors also thank Dr. Tchuifon Donald and Dr. Bopda Aurelien for their contribution.

References

[1] S. Suresh, V. C. Srivastava, and I. M. Mishara, "Adsorption of hydroquinone in aqueous solution by granulated activated carbon," *Journal of Environnement Engineering*, vol. 137, pp. 1–12, 2011.

[2] D. A. Blanco-Martínez, L. Giraldo, and J. C. Moreno-Piraján, "Effect of the pH in the adsorption and in the immersion enthalpy of monohydroxylated phenols from aqueous solutions on activated carbons," *Journal of Hazardous Materials*, vol. 169, no. 1-3, pp. 291–296, 2009.

[3] N. N. Patricia, K. Théophile, T. T. D. Raoul, D. Giscard, B. M. M. Roger, and A. S. Gabche, "Non-linear regression, a better approach for the optimisation of hydroquinone, resorcinol and catechol adsorption by chemically activated carbon based on monkey kola (cola lepidota k. schum) waste," *Chemical Science International Journal*, vol. 25, no. 1, pp. 1–18, 2018.

[4] M. Zhang, C.-y. Ge, Y.-f. Jin et al., "Sensitive and simultaneous determination of hydroquinone and catechol in water using an anodized glassy carbon electrode with polymerized 2-(phenylazo)," *Journal of Chemistry*, vol. 2019, Article ID 2327064, 10 pages, 2019.

[5] S. Rengaraj, S.-H. Moon, R. Sivabalan, B. Arabindoo, and V. Murugesan, "Agricultural solid waste for the removal of organics: adsorption of phenol from water and wastewater by palm seed coat activated carbon," *Waste Management*, vol. 22, no. 5, pp. 543–548, 2002.

[6] INRS, *Base de données Fiches Toxicologiques*, INRS, Quebec City, Canada, hydroquinone edition, 2006.

[7] INRS, *Base de données Fiches Toxicologiques*, INRS, Quebec City, Canada, Résorcinol edition, 2018.

[8] S. E. Agarry, A. O. Durojaiye, R. O. Yusuf, M. O. Aremu, B. O. Solomon, and O. Mojeed, "Biodegradation of phenol in refinery wastewater by pure cultures of Pseudomonas aeruginosa NCIB 950 and Pseudomonas fluorescence NCIB 3756," *International Journal of Environment and Pollution*, vol. 32, no. 3, 2008.

[9] R. Subramanyam and I. M. Mishra, "Co-degradation of resorcinol and catechol in an UASB reactor," *Bioresource Technology*, vol. 99, no. 10, pp. 4147–4157, 2008.

[10] A. Garg, I. M. Mishra, and S. Chand, "Oxidative phenol degradation using non-noble metal based catalysts," *Clean-Soil, Air, Water*, vol. 38, no. 1, p. NA, 2010.

[11] E. Ouabou, A. Anouar, and S. Hilali, "Élimination des polluants organiques dans la margine d'huile d'olive par filtration sur colonne d'argile et sciure de bois d'eucalyptus," *Journal of Applied Biosciences*, vol. 75, no. 1, pp. 6232–6238, 2014.

[12] S. G. Kouassi, P. A. Grah, K. D. Bini et al., "Contribution à l'étude de quatre charbons activés à partir des coques de noix de coco," *Afrique Science*, vol. 12, no. 5, pp. 229–245, 2016.

[13] B. Sawadogo, Y. Konaté, G. Lesage et al., "Brewery wastewater treatment using MBR coupled with nanofiltration or electrodialysis: biomass acclimation and treatment efficiency," *Water Science and Technology*, vol. 77, no. 11, pp. 2624–2634, 2018.

[14] B. Davoud and J. Ali, "Biosorption of Phenol using dried Rice husk biomass: kinetic and equilibrium studies," *Der Pharma Chemica*, vol. 8, no. 6, pp. 96–103, 2016.

[15] M. J. Ahmed and S. K. Dhedan, "Equilibrium isotherms and Kinetics modeling of methylene blue adsorption on agricultural Wastes-based activated carbons," *Fluid Phase Equilibria*, vol. 317, pp. 9–14, 2012.

[16] N. Fayoud, S. A. Younssi, S. Tahiri, and A. Albizane, "Etude cinétique et thermodynamique de l'adsorption de bleu de méthylène sur les cendres de bois (Kinetic and thermodynamic study of the adsorption of methylene blue on wood ashes)," *Journal of Materials and Environmental Sciences*, vol. 6, no. 11, pp. 3295–3306, 2015.

[17] T. Li, Y. He, and X. Peng, "Efficient removal of tetrabromobisphenol A (TBBPA) using sewage sludge-derived biochar: adsorptive effect and mechanism," *Chemosphere*, vol. 251, Article ID 126370, 2020.

[18] T. Robinson, G. Mcmullan, R. Marchant, and P. Nigam, "Remediation of dyes in textile effluent: a critical review on current treatment technologies with a proposed alternative," *Bioresource Technology*, vol. 77, no. 3, pp. 247–255, 2001.

[19] R. Shanmugavalli, P. S. S. Shabudeen, R. Venckatesh et al., "Uptake of Pb (II) ion from aqueous solution using silk cotton hull carbon: an agricultural waste biomass," *E-Journal of Chemistry*, vol. 3, no. 4, pp. 218–229, 2006.

[20] R. S. Alwi, R. Gopinathan, A. Bhowal, and C. Garlapati, "Adsorption characteristics of activated carbon for the reclamation of eosin Y and indigo carmine colored effuents and new isotherm model," *Molecules*, vol. 25, no. 24, pp. 6014-6015, 2020.

[21] P. Sudamalla, P. Saravanan, and M. Matheswaran, "Optimisation of operating parameters using response surface methodology for adsorption of crystal violet by activated carbon prepared from mango kernel," *Environment Research*, vol. 22, no. 1, pp. 1–7, 2012.

[22] S. Debnath, N. Ballav, A. Maity, and K. Pillay, "Development of a polyaniline-lignocellulose composite for optimal adsorption of Congo red," *International Journal of Biological Macromolecules*, vol. 75, pp. 199–209, 2015.

[23] C. D. Atemkeng, G. S. Anagho, T. F. R. Tagne, A. L. Amola, A. Bopda, and T. Kamgaing, "Optimization of 4-nonylphenol adsorption on activated carbons derived from safou seeds using response surface methodology," *Carbon Trends*, vol. 4, 2021.

[24] V. O. Shikuku, C. O. Kowenje, and F. O. Kengara, "Errors in parameters estimation using linearized adsorption isotherms: sulfadimethoxine adsorption onto kaolinite clay," *Chemical Science International Journal*, vol. 23, no. 4, pp. 1–6, 2018.

[25] A. Bopda, T. D. R. Tchuifon, N. G. Ndifor-Angwafor, G. Doungmo, and S. G. Anagho, "Non-linear equilibrium and kinetic study of the adsorption of 2,4-dinitrophenol from aqueous solution using activated carbon derived from a olives stones and cotton cake," *African Journal of Environmental Science and Technology*, vol. 13, no. 9, pp. 365–380, 2019.

[26] T. Kamgaing, G. Doungmo, F. M. Melataguia Tchieno, J. J. Gouoko Kouonang, and K. J. Mbadcam, "Kinetic and isotherm studies of bisphenol A adsorption onto orange albedo (Citrus sinensis): sorption mechanisms based on the main albedo compenents vitamin C, flavones glycosides and caortenoids," *Journal of Environmental Science and Health, Part A*, vol. 52, no. 8, pp. 757–769, 2017.

[27] C. S. Ngakou, G. S. Anagho, and H. M. Ngomo, "Non-linear regression analysis for the adsorption kinetics and equilibrium isotherm of phenacetin onto activated carbons," *Current Journal of Applied Science and Technology*, vol. 36, no. 4, pp. 1–18, 2019.

[28] L. A. Amola, T. Kamgaing, D. R. T. Tchuifon, C. D. Atemkeng, and S. G. Anagho, "Activated carbons based on shea nut shells (vitellaria paradoxa): optimization of preparation by chemical means using response surface methodology and physico-chemical characterization," *Journal of Materials Science and Chemical Engineering*, vol. 08, no. 08, pp. 53–72, 2020.

[29] S. K. V. Nayarana, P. King, R. Gopinadh, and V. Sreeiakshmi, "Response surface optimization of dye remolval by using waster prawn shells," *International Journal of Chemical Sciences and Applications*, vol. 2, pp. 186–193, 2011.

[30] R. Arunachala and G. Annadurai, "Optimizred response surface methodology for adsorption of dyestuff from aqueous solution," *Journal of Environmental Science and Technology*, vol. 4, no. 1, pp. 65–72, 2010.

[31] S. Lagergren, "About the theory of so called adsorption of soluble substances," *KulingasvenskaVetenskapsakademiensHandlingar*, vol. 24, pp. 1–39, 1898.

[32] Y. S. Ho and G. McKay, "Pseudo-second order model for sorption process," *Process Biochemistry*, vol. 34, no. 5, pp. 451–465, 1999.

[33] S. H. Chien and W. R. Clayton, "Application of Elovich equation to the kinetics of phosphate release and sorption in soils," *Soil Science Society of America Journal*, vol. 44, no. 2, pp. 265–268, 1980.

[34] W. J. Weber and J. C. Morris, "Kinetic of adsorption of carbon from solution," *Journal of the Sanitary Engineering Division*, vol. 89, no. 2, pp. 31–59, 1963.

[35] B. Al Duri and G. McKay, "Basic dye adsorption on carbon using a solid phase diffusion model," *The Chemical Engineering Journal*, vol. 38, no. 1, pp. 23–31, 1988.

[36] D. A.O, A. P. Olalekan, A. M. Olatunya, O. Dada, and F. ''Langmuir, "Temkin and dubinin–radushkevich isotherms studies of equilibrium sorption of Zn2+ unto phosphoric acid modified rice husk," *IOSR Journal of Applied Chemistry*, vol. 3, no. 1, pp. 38–45, 2012.

[37] M. I. Temkin and V. Pyzhev, "Kinetics of ammonia synthesis on promoted iron catalyst," *Acta Physicochimica*, vol. 12, pp. 327–356, 1940.

[38] N. Ayawei, A. N. Ebelegi, and D. Wankasi, "Modelling and interpretation of adsorption isotherms," *Journal of Chemistry*, vol. 2017, Article ID 3039817, 11 pages, 2017.

[39] S. Rangabhashiyam, N. Anu, M. S. Giri Nandagopal, and N. Selvaraju, "Relevance of isotherm models in biosorption of pollutants by agricultural byproducts," *Journal of Environmental Chemical Engineering*, vol. 2, no. 1, pp. 398–414, 2014.

[40] M. Katell, *Méthode d'analyse de données en régression non linéaire*, pp. 7-8, Hall, Hoboken, NJ, USA, 2013.

[41] M. A. Hossain, H. H. Ngo, and W. Guo, "Introduction of microsoft excel SOLVER function-spreadsheet method for isotherm and kenetic modeling of metals biosorption in water and wastewater," *Journal of Water Sustainability*, vol. 3, no. 4, pp. 223–237, 2013.

[42] C. Chen, "Evaluation of equilibrium sorption isotherm equations," *The Open Chemical Engineering Journal*, vol. 7, no. 1, pp. 24–44, 2013.

[43] K. Y. Foo and B. H. Hameed, "Insights into the modeling of adsorption isotherm systems," *Chemical Engineering Journal*, vol. 156, no. 1, pp. 2–10, 2010.

[44] M. Can, "Studies of the kinetics for rhodium adsorption onto gallic acid derived polymer: the application of nonlinear regression analysis," *Acta Physica Polonica A*, vol. 127, no. 4, pp. 1308–1310, 2015.

[45] X. Jing, Y. Zhu, and Z. Yong-Fa, "Elimination of bisphenol. A from water via graphene oxide adsorption," *Acta Physico-Chimica Sinica*, vol. 29, no. 04, pp. 829–836, 2013.

[46] F. Sakr, A. Sennoui, M. Elouardi, M. Tamimi, and A. Assabbane, "Etude de l'adsorption du bleu de méthylène sur un biomatériau à base de cactus," *Journal of Materials and Environmental Sciences*, vol. 6, pp. 397–406, 2015.

[47] H. N. Tran, Y.-F. Wang, S.-J. You, and H.-P. Chao, "Insights into the mechanism of cationic dye adsorption on activated charcoal: the importance of $\pi-\pi$ interactions," *Process Safety and Environmental Protection*, vol. 107, pp. 168–180, 2017.

[48] S. D. B. Maazou, H. I. Hima, M. M. Malam Alma, Z. Adamou, and I. Natatou, "Elimination du chrome par du charbon actif elabore et caracterise a partir dela coque du noyau de Balanites aegyptiaca," *International Journal of Brain and Cognitive Sciences*, vol. 11, no. 6, pp. 3050–3065, 2017.

[49] I.-H. T. Kuete, D. R. T. Tchuifon, G. N. Ndifor-Angwafor, A. T. Kamdem, and S. G. Anagho, "Kinetic, isotherm and thermodynamic studies of the adsorption of thymol blue onto powdered activated carbons from Garcinia cola nut shells impregnated with H3PO4 and KOH: non-linear regression analysis," *Journal of Encapsulation and Adsorption Sciences*, vol. 10, no. 01, pp. 1–27, 2020.

[50] C. Ding, Y. Li, Y. Wang et al., "Highly selective adsorption of hydroquinone by hydroxyethyl cellulose functionalized with magnetic/ionic liquid," *International Journal of Biological Macromolecules*, vol. 107, pp. 957–964, 2018.

[51] D. Ajifack, J. Ghogomu, T. Noufame, J. Ndi, and J. Ketcha, "Adsorption of Cu (II) ions from aqueous solution onto chemically prepared activated carbon from theobroma cacoa British," *British Journal of Applied Science & Technology*, vol. 4, no. 36, pp. 5021–5044, 2014.

[52] D. Balarak, M. Zafariyan, C. A. Igwegbe, K. K. Onyechi, and J. O. Ighalo, "Adsorption of acid blue 92 dye from aqueous solutions by single-walled carbon nanotubes: isothermal," *Environmental Processes*, vol. 8, no. 2, pp. 869–888, 2021.

[53] A. Tyagi, S. Das, and V. C. Srivastava, "Removal of toxic hydroquinone : comparative studies on use of iron impregnated gra nular activated carbon as an adsorbent and catalyst," *Environmental Engineering Research*, vol. 24, no. 3, pp. 474–483, 2019.

[54] Z. U. Ahmad, Q. Lian, M. E. Zappi, P. R. Buchireddy, and c D. D. Gang, "Adsorptive removal of resorcinol onto surface modified ordered mesoporous carbon: kinetics and equilibrium," *Study Environmental Progress & Sustainable Energy*, vol. 12, 2018.